# A Computational Investigation for the Chiral Chromatographic Separation of Benzimidazole Type Sulphoxides

**Hatice ÖZDEMİR CAN**
*Chemistry Department, Mersin University, 33342 Mersin-TURKEY*
*e-mail: haticecan@mersin.edu.tr*

The computational study of chromatographic separations has become increasingly important in recent years. It supplies useful information about the mechanism of chromatographic separations and the design of stationary phases. In this study, the chromatographic separations of chiral benzimidazole type sulphoxides were analysed by utilising computational tools. The chiral separation mechanism of these compounds was analysed by molecular modelling methods. Molecular mechanics (MM+) were used as force field calculations. The separation factors and elution orders were determined from the interaction energies. Furthermore, the matrix effect on separation was investigated.

**Key Words:** Molecular modelling, sulphoxides, molecular, mechanics, chiral separation, chromatography.

## Introduction

The resolution of enantiomers by chromatography or columns packed with one enantiomer of a chiral substance is possible, but selecting which one for use or even designing such stationary phases represents a real problem for the pharmaceutical industry. Computational chemistry approaches may have a useful role to play in the design or choice of column stationary phases for the resolution of a mixture of enantiomers which in turn would allow one to investigate the physiological properties of pure isomers.

The major developments in the field of chiral separations were reviewed by Ward[1]. This review includes applications in chiral separations and developments between 1997 and 1999.

Methods of predicting the elution order and separation selectivity of enantiomers suggest a computation of the energetic differences related to interactions between the selector and selectand for both enantiomers to be separated[2]. The procedures involve the generation of the most possible diastereomeric associations or complexes, chiral selector and enantiomeric solute and then approximating the conformations to the global energetic minima, which are used to estimate the enantioselectivity for the studied analytes.

The initial utilisation of atomistic molecular modelling in the area of chiral chromatography was achieved by Weinstein et al.[3]. They proposed a molecular model which accounts for stereoselective interactions within a series of chiral secondary amides.

553

The majority of computational works have been carried out by Lipkowitz and his group for understanding the enantioselectivity of brush-type stationary phases. The earlier investigations were initiated by them[4]. They started to analyse the physicochemical properties of chiral stationary phases (CSPs) before developing a chiral recognition model. For this purpose, they concentrated on the structural and electronic features of the Pirkle CSP using computational techniques[5−10]. The conformational flexibility of CSPs make these phases more effective and allow maximum binding to complementary sites on the analyte.

Lipkowitz et al. provided a computational protocol for the analysis of optical analytes on CSP used in chromatography[11]. Employing this approach, they calculated the interaction energies between the CSP and analyte molecules. They successfully predicted the elution order and separation factors[12].

The work of Topiol and co-workers does not comprise another methodology for generating diastereomeric complexes, but is of interest because the distinct types of interactions observed in such complexes were calculated using different levels of approximation. Taking the diastereomeric complexes proposed by Pirkle, based on NMR-NOE studies[13], Topiol was able to quantify the interaction energy contributions of hydrogen bonds and $\pi - \pi$ interactions separately[14]. Simple MM was used to compute the conformational minima of the CSP and analyte, and (models of) the diastereomeric complexes were treated with both ab initio (STO-3G basis set)[15] and semi-empirical (AM1) QM[16] methods. Topiol et al. concluded that hydrogen bond(s) must be regarded as the main stabilising interaction, whereas the $\pi - \pi$ interactions are relatively weak and do not contribute to chiral discrimination. The calculated (AM1) energy difference $\Delta\Delta G(g)$ of 0.8 kcal/mol and the configuration of the computed complexes were in agreement with experimental data[14,17].

To examine pictorially the role of entropic effects in these transient diastereomeric complexes, Sabio and Topiol performed extensive MD simulations on the system studied previously using the AM1 approach[18]. The results made clear that the geometry of the diastereomeric complexes is not affected significantly by entropic effects.

Still and Rogers evaluated the distribution of conformers of the analyte and CSP (bonding tert-butyloxycarbonyl [BOC] derivatives of amino acids to a butyl spacer on silica) employing a MM2 force field[19]. The calculations predicted correctly the elution order as well as the relative resolving powers of the two bonded phases. Replacing the n-butyl spacer chain with a methyl, ethyl, or n-propyl group confirmed the importance of chain length.

Quantitative structure-enantioselective retention relationship (QSERR) equations were used to assist molecular modelling experiments designed to investigate the chiral separation mechanism[20].

In this study, chiral separations of benzimidazole type sulphoxides (Figure 1) on a Pirkle column (Figure 2) were analysed by molecular modelling techniques. The model developed by Edge[21] was used for computing the interaction energies between the CSP and analyte molecules. The separation factors and elution orders were predicted successfully. The effect of the silica matrix and the steric bulk of the analyte molecule were discussed.
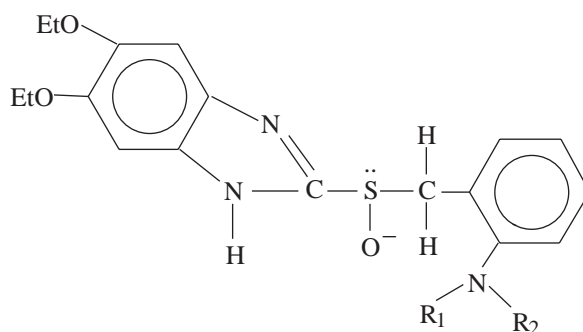
**Figure 1.** The sulphoxide structure as analyte molecule: Benzenamine, 2[[5,6- diethoxy-1H-benzimidazole-2yl) sulfinyl]methyl.
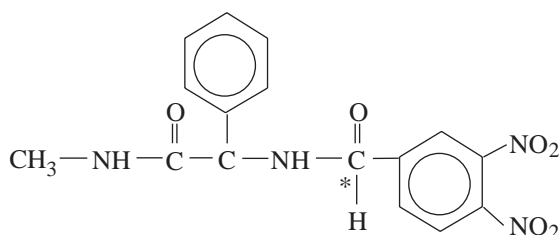
**Figure 2.** The Pirkle-type chiral stationary phase: (S)-N-(3,5-dinitrobenzoyl phenyl glycine-N'-methylamide.

## Method

Geometric optimisations of solute and CSP molecules were achieved by performing molecular mechanics (MM+) calculations with HyperChem[22]. Molecular mechanics geometry optimisation was accomplished using the Polak-Ribiere algorithm with the RMS gradient of 0.001 kcal/Å mol as a convergence condition.

The polarisability and refractivity of solute molecules were calculated by the ChemPlus program, which is a part of the HyperChem package.

The establishment of a model for the investigation of chromatographic separation in a chromatographic column demands some approximations because of the huge computational time. One of the approximations concerns the formation of the diastereomeric complex that was considered as a 1:1 complex between the analyte and stationary phase molecule. The rate of complex formation is equal for R and S enantiomers.

The silica support is supposed to have no influence on the recognition of enantiomers. The chiral part of the CSP is attached to a carrier material which is generally silica gel via a spacer such as a $(CH_2)_n$ chain assumed to be inactive. The spacer chain had been cut off to a methyl group in our calculations.

Even diastereomers possess different solvation free energies and the solvent can sometimes influence the retention orders. In this study, however, the solvent or mobile phase has been omitted. Hence the model consists of a gas-phase complex. Naturally, both enantiomers of the analyte in the solvent are solvated similarly; however, solvation of the transient diastereomeric complexes can be different. This difference is

obvious if the solvent partakes in hydrogen bonding. Experimental studies indicated that the solvent does not contribute to the chiral separation[23].

# The Model

This model contributed substantially to the development of an extensive method to generate diastereomeric complexes. One method of finding the most auspicious binding sites between the CSP and R or S enantiomers of analyte molecule is to perform a grid search. The home-made program, which is prepared in Visual Basic language, is used to perform the grid search method. Geometry optimisations and single-point calculations are performed using HyperChem. The connection between the home-made program and HyperChem is provided by dynamic data exchange (DDE) links in the HyperChem package. The DDE links system employs the messages for the start of another application, to establish a transmissions channel with another application, to send data, and to request and receive data; and to get information automatically, when it is updated.

In the grid search method, complexes are sampled systematically using minimum energy conformers of the CSP and analyte. As a consequence of the grid search, all possible configurations and orientations of the complexes formed between the two molecules are computed. In essence, this signifies that several thousand orientations of the two molecules have to be analysed to determine a reasonable value for the lowest energies available to the CSP and analyte. The geometry optimisation procedure which reorientates the molecules into the nearest local energy minima assists the grid search method. The sampling of several thousand configurations and orientations of the complex is achieved by utilising the home-made program. Each movement of the analyte on the CSP surface is sampled while the complex is being formed between the analyte and CSP. As metioned above, the geometry optimisation procedure is applied to each complex to obtain the lowest energies and reorientate the complex into the nearest local minima. The cylindrical coordinates set the starting grid which is stepwise motion of the analyte on every side of the CSP. The position of the enantiomer molecule employed in this grid search analysis (Fig. 3) with respect to the CSP is defined by two coordinates, $\theta$ and Z. $\theta$ is the rotation angle of the analyte molecule on CSP, and it increases $20°$ at each step.

Before the motion of the analyte on the CSP, the home-made program read the initial coordinates of CSP and analyte. At the beginning of the analyte movement, the analyte is moved on the CSP surface with a $20°$ rotation angle at the initial coordinate of CSP. This rotation with $20°$ increments is completed until a $360°$ rotation hour is finished. Once the $360°$ rotation hour is achieved, the analyte is flipped over by $180°$ to allow the interaction of the rear side of the analyte with the CSP in the same way. After one $360°$ rotation hour, the analyte molecule moves to the next coordinates of the CSP. These movements on the CSP take place along the z-coordinate of the CSP. The z-coordinate is choosen as the analyte's motion direction and path. Z is the z-coordinate of the CSP.

Figure 3 shows a schematic diagram of the model which represents the movement of the analyte around the CSP.

At the end of running this program, several thousand pieces of data which include the total interaction energies, initial and final coordinates and rotation angles were recorded. These raw data were used to establish the three-dimensional potential energy surface graphs. Total energy was converted to free energies by applying the Boltzmann distribution equation. Boltzmann distribution over all the computed interaction energies as a weighted average is utilised to find out the binding ability of the analyte to the CSP.
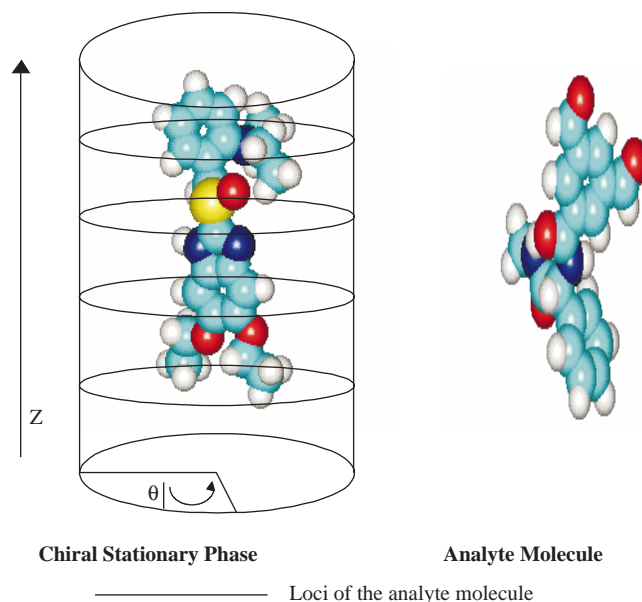
**Chiral Stationary Phase**          **Analyte Molecule**

—————————— Loci of the analyte molecule

**Figure 3.** Schematic diagram of the computational model [ref. 21].

Since computational time is the most important point in this kind of computations, force field calculations are employed to describe the interactions formed between the atoms rather than using ab-initio or semi-empirical calculations which generate more data and greatly increase the computational time.

# Results and Discussion

Theoretical and experimental results indicate that the chiral chromatographic separation of benzimidazole type sulphoxides enantiomers, solute I and II, on a Pirkle-type column display very different separation behaviour.

## Intermolecular potential energy surfaces for solute-CSP complexes

Figures 4, 5, 8 and 9 contain the results of the grid search method that display the intermolecular potential energy surfaces calculated by MM+ calculations. The intermolecular potential surfaces provide information about where the analyte is most likely to bind around the CSP[24]. The intermolecular energy between the CSP and analyte is also called column-averaged interaction energy. The column-averaged interaction energy, E, depends on the shape of the analyte and CSP, and the orientation of the two relative to one another. Many CSP molecules are flexible organic molecules that can give multiple conformations each of which can interact with the analyte in a different way. Solute I and II enantiomers also are not rigid molecules that can adopt multiple conformation to bind to the CSP in different conformations.
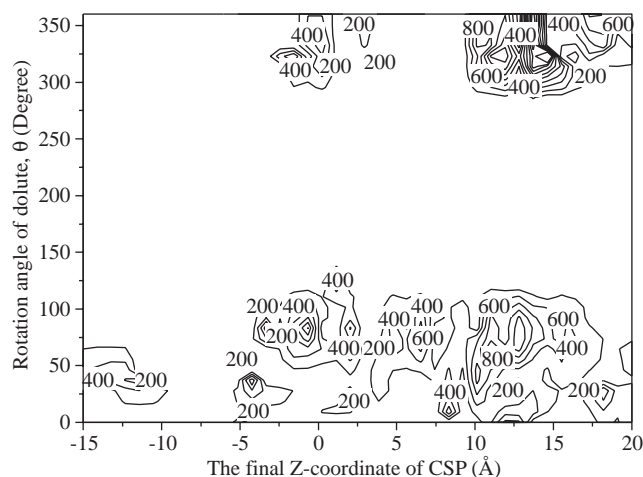
**Figure 4.** Intermolecular potential energy surface for the RR diastereomeric complex formed from binding solute I to the CSP. (The intermolecular energy unit is kcalmol$^{-1}$).
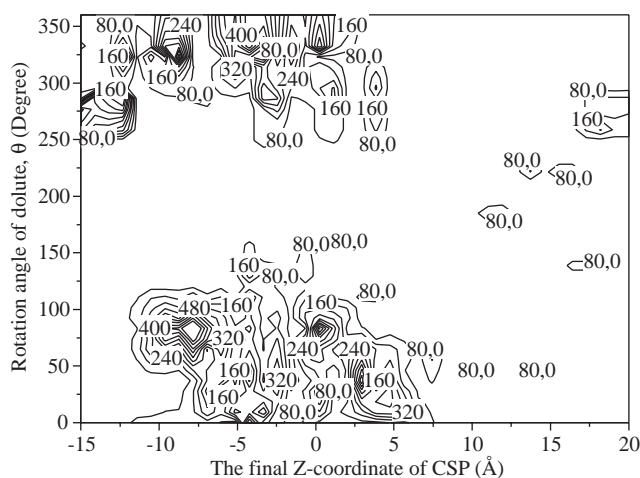


**Figure 5.** Intermolecular potential energy surface for the RS diastereomeric complex formed from binding solute I to the CSP. (The intermolecular energy unit is kcalmol$^{-1}$).

The interactions of CSP with the analyte molecules can occur via hydrogen bonding, $\pi - \pi$ interactions, dipole-dipole stacking, hydrophobic, charge-transfer interactions etc. As a result of these interactions, a diastereomeric complex is formed between the CSP and analyte.

The classical chiral recognition mechanism model involves three simultaneous interactions between the CSP and at least one of the enantiomers[25]. This model is called "three-point interactions". Three-point interactions typically involve only a $\pi - \pi$ interaction, hydrogen bondings and dipole stacking. When the analyte is docked in this CSP, there is a potential for three simultaneous hydrogen bonding interactions. These hydrogen bonds are shown in Figure 6.
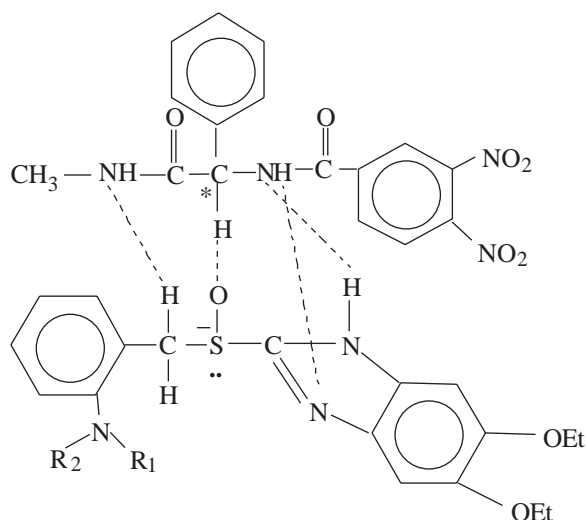
**Figure 6.** Proposed mechanism of binding displaying hydrogen bonding sites for the CSP and solute.

Although the two enantiomers form similar interactions with CSP, diastereomeric analyte-CSP complexes diverge in their stabilities emerging to chiral discrimination. The energy difference between the (R)Solute-CSP and (S)Solute-CSP complexes stem from different orientations of solute enantiomers for binding to the CSP, while they make the same interaction. It was concluded that both enantiomers of solute I can create the same molecular interactions as hydrogen bonding. The distinction for the formation of that hydrogen bond is the orientation of the analyte for binding to the CSP (Figure 7).
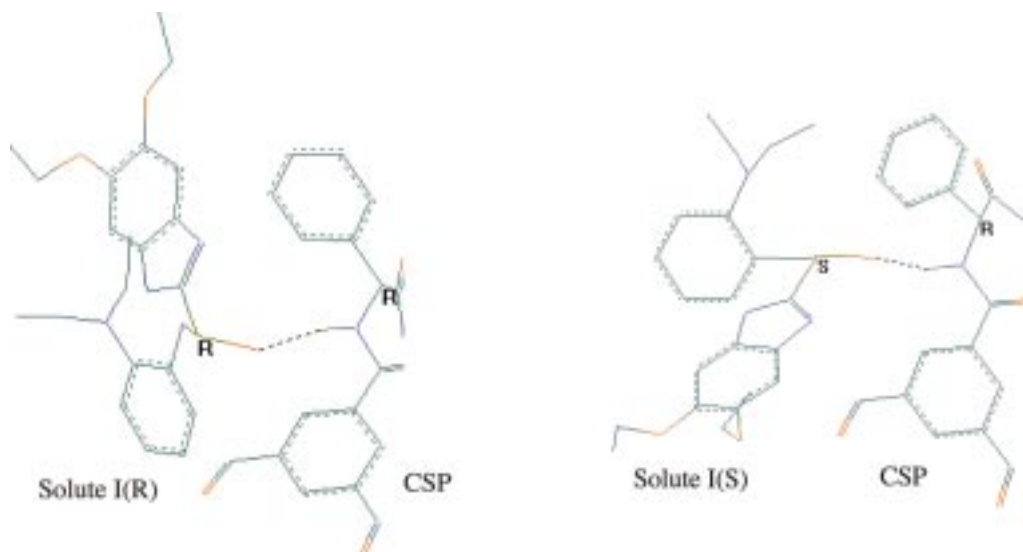


**Figure 7.** The same hydrogen bond between the solute I enantiomers and CSP.

When solute enantiomers bind to CSP via a hydrogen bond, solute enantiomer and CSP conformationally adjust to each other to maximise the interactions and, thereby, the stabilities of the diastereomeric complexes. It is this step that produces the different stabilities of (R)Solute I- CSP and (S)Solute I-CSP complexes and finally the observed enantioselective separation. It is deduced that chiral recognition arises from the orientation of sulphoxide molecules during the complexation with the CSP. The intermolecular potential energy surfaces of Solute I-CSP complexes (Figures 4 and 5) also reflect those insights on the

enantioseparation mechanism. As seen from Figures 4 and 5, while high energetic interactions between the (R)Solute I-CSP take place on 5-7.5 Å of the z-coordinate of the CSP, high energetic interactions for (S)Solute I with CSP occur in a different part of the map, (-5)-(-7.5) Å of the z-coordinate of the CSP. In the case of solute II-CSP interactions, high energetic interactions arise on generally a similar part of the CSP (Figures 8 and 9).

The favoured binding sites around the CSP can be predicted by evaluating the intermolecular energy at each latitude and longitude as the analyte rotates and flipps over the CSP, i.e. as a function of $\theta$ and Z, defined earlier. An enormous number of configurations have been sampled for the entire complex formed between the CSP and the analyte for each configuration, which means at each $\theta$ and Z.

These potential energy surfaces are interestingly identical but diversity exists in the binding sites of the CSP (Figures 4 and 5). For solute I(S)-CSP complex, broad and shallow binding regions on the CSP preferred by solute I(S) take place between 7.5 Å and 20 Å of CSP's Z-coordinate (Figure 5). In contrast, as seen in Figure 4, the potential energy surface of solute I(R)-CSP complex does not indicate the same magnitude of broad and shallow areas and these shallownesses do not occur at the same values of Z and $\theta$. The high peaks on the intermolecular potential energy surfaces are located in different regions as shown in Figures 4 and 5. These high peaks correspond to strong molecular interactions such as $\pi$-donor-acceptors, hydrogen bonding and steric interactions between the sulphoxide molecule and CSP.

In the case of solute II enantiomers, the enantioselectivity was decreased. Figures 8 and 9 present the interactions of solute II enantiomers with the CSP. The well pronounced binding sites are at Z values of -10 Å and 15 Å and, $\theta$ values of 150 °-200 ° for both enantiomers. As seen from Figures 8 and 9, both enantiomers of solute II prefer similar sites of the CSP. The differences between the binding sites of CSP for R- and S-solute II are not very large. While the differences in preferred sites of CSP are increased, chiral recognition is improved.
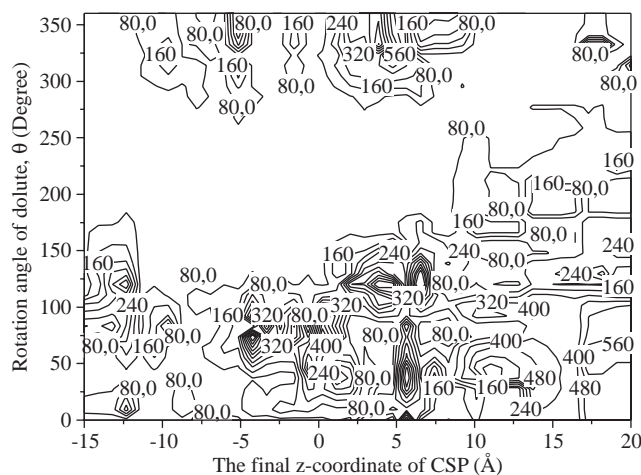


**Figure 8.** Intermolecular potential energy surface for the RR diastereomeric complex formed from binding solute II to the CSP. (The intermolecular energy unit is kcalmol$^{-1}$).
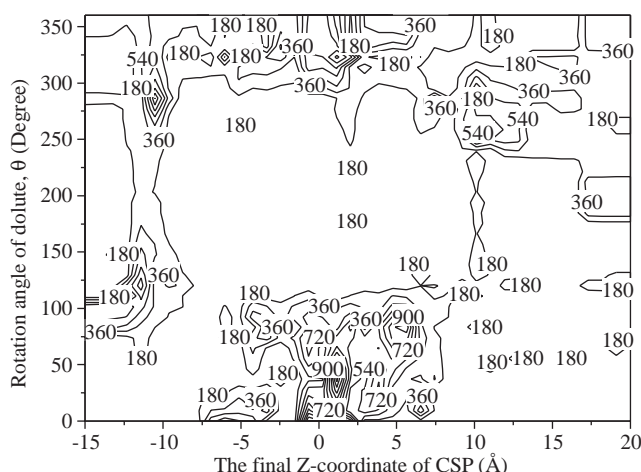
**Figure 9.** Intermolecular potential energy surface for the RS diastereomeric complex formed from binding solute II to the CSP. (The intermolecular energy unit is kcalmol$^{-1}$).

The bonding conformation of (R)-sulphoxide I is approximately 3.95 kcalmol$^{-1}$ higher in energy than that of (S)-sulphoxide I (Table 1). The theoretical enantioselectivity arising from this energy difference can be estimated using the equation[26]

$$\Delta\Delta G = -RT\ln\alpha$$

$\Delta\Delta$G is the energy difference obtained by substracting the value of the RS complex from that of the RR complex.

**Table 1.** The effects of matrix on the separation of solute I.

| Steric factor, K | Interaction energy/kJmol$^{-1}$ | | $\Delta(\Delta\overline{G})$/kJmol$^{-1}$ | $\alpha$ |
|:---:|:---:|:---:|:---:|:---:|
| K | $\underline{S}$ | $\underline{R}$ | | |
| 0.00 | 203.82 | 207.76 | 3.95 | 5.06 |
| 0.005 | 235.89 | 180.51 | -55.37 | no separation |

Experimental[27] and theoretical show present that solute I has the highest separation factor. Table 1 and 3 contain the column-averaged interaction energies for two compounds with the CSP and also present the theoretical separation factors for the two pairs of enantiomers. The reasons for the better separation of solute I may be explained by the intermolecular potential energy map of solute I-CSP diastereomeric complex (Figures 4 and 5), the polarisability of the amine group attached to the phenyl ring and the refractivity values of solutes (Table 4). The energy of each diastereomeric complex depends on the shape of the CSP, the shape of the analyte, and the orientation of these two relative to one another.

**Table 2.** Experimental[27] results of the separation of sulphoxides on two CSPs which are two different spacer groups attached to the silica (the spacer group [(CH2)4]; the spacer group [(CH2)11].

| Compound | Pirkle column [(CH$_2$)$_4$] | Pirkle-type column[(CH$_2$)$_{11}$] | | |
|:---:|:---:|:---:|:---:|:---:|
| | | k$_1$ | k$_2$ | $\alpha$ |
| solute I | no separation | 6.60 | 8.01 | 1.21 |
| solute II | no separation | 10.41 | 11.60 | 1.11 |

**Table 3.** The effects of the matrix on the separation of solute II.

| Steric factor, K | Interaction energy/kJmol$^{-1}$ | | $\Delta(\Delta\overline{G})$/kJmol$^{-1}$ | $\alpha$ |
|:---:|:---:|:---:|:---:|:---:|
| K | S | R | | |
| 0.00 | 251.65 | 247.35 | 4.31 | 5.86 |
| 0.005 | 252.68 | 248.29 | 4.39 | 6.07 |
| 0.020 | 254.17 | 251.13 | 3.04 | 3.49 |
| 0.025 | 254.68 | 252.09 | 2.59 | 2.89 |
| 0.030 | 255.18 | 253.06 | 2.13 | 2.39 |
| 0.035 | 255.68 | 254.01 | 1.67 | 1.98 |
| 0.040 | 256.18 | 254.98 | 1.21 | 1.64 |
| 0.050 | 257.19 | 256.92 | 0.27 | 1.12 |
| 0.060 | 258.20 | 258.88 | -0.68 | no separation |

The analytes are separable on Pirkle-type chiral stationary phases which are the N-(3,5-dinitrobenzoyl) derivatives of $\alpha$-amino acids containing $\theta$ donor functionality and dipolar $\pi$-groups conformationally influenced by the stereogenic centres. Generally, the analyte contains basic sites that can act as a hydrogen bond acceptor, indeed the presence of acidic hydrogens in the analyte may sometimes improve separability as well[28]. Solute I is a strong $\pi$-electron donor due to the benzimizadole ring with two electron donating groups such as ethoxy and the phenyl ring with the amine group which has two ethyl attachments.

The magnitude of molecular polarisability seems to improve chiral discrimination. Substituents with electron-accepting properties (such as $NO_2$) will favour a more conjugated electron system. The amine group of solute I has the highest polarisability (Table 4). The capability of electron delocalisation seems to improve the chiral discrimination of benzimidazole sulphoxides.

**Table 4.** Refractivity and polarisability values of the amine group on the sulphoxide molecule.

| Molecular descriptor | solute I (R)-(R)- | solute I (S)-(S)- | solute II (R)-(R)- | solute II (S)-(S)- |
|:---:|:---:|:---:|:---:|:---:|
| Refractivity of amine group($\text{Å}^3$) | 24.51 | 24.51 | 15.53 | 15.53 |
| Polarisability of amine group | 9.08 | 9.08 | 5.41 | 5.41 |

The effect of the steric bulk of the $-N(Et)_2$ moiety on chiral separation was observed. Previous studies[28-30] indicated that the size of the substituent at the sterogenic centre affects $\alpha$. Generally, the $\alpha$ value increase with the increases in substituent size. The resolution of the enantiomers of benzimidazole sulphoxides appears to be strongly dependent on the presence of substituents in the amino group attached to the phenyl.

The stability of complexes is governed by the orientation of the sulphoxide molecule for binding to the CSP. While considerably different orientations of solute I enantiomers are observed due to the steric effect of $-N(Et)_2$ moiety near the stereogenic centre, smaller orientations of solute II enantiomers occurred.

## Matrix Effect

The calculated separation factor, $\alpha$, is higher than that obtained experimentally. It can be explained by the absence of the steric effect of the silica matrix. As indicated in Tables 1 and 3, the steric hindrance factor, K, increased from 0.00, which meant no steric effect, to 0.005 or 0.06, up to which no separation is

observed. When the steric effect factor is increased, the mean interaction energies are decreased. It can be concluded that a higher steric effect of the matrix to fewer binding sites allows discrimination between two enantiomers, hence resulting in more difficult separation. The bonding of the active part of the CSP to the matrix is one of the key factors which must be considered carefully in the designing of CSPs. Details of the calculations of the matrix effect are given elsewhere[21].

The most important aspect from our calculations is the prediction of which optical isomer is most retained on the column. The most retained enantiomer is the one for which the value of $\Delta G$ is the most negative. The total interaction energies summed over all orientations of all complexes predict that the S enantiomer of solute I is retained on the column more than the R enantiomer. This agrees with the experiment. There are many assumptions made in these calculations, for example the elimination of the spacer chain connecting the CSP to the silica. If the steric hindrance factor is considered, the equation of $\Delta G$ includes the steric hindrance factor, K, which is between the matrix and the analyte molecule. As shown in Table 1, if there is no steric hindrance, separation is increased. Solute I has a more bulky structure than the others. Therefore, the small steric hindrance between the matrix and solute I causes the disappearance of separation.

The R enantiomer of solute II is retained more on the column, because the R enantiomer has a smaller interaction energy than the S enantiomer. Solute II is less bulky than solute I. Even if the steric factor is higher than that in Table 3, separation can still occur.

# Conclusion

The separation mechanism of benzimidazole type sulphoxide on a Pirkle-type CSP was investigated by molecular modelling techniques. The chiral separation is initiated by the "three-point interactions". The three-point interactions such as hydrogen bonding, $\pi - \pi$ interactions and dipole stacking are required for binding to the stationary phase. The steric bulkiness around the stereogenic centre of the analyte during the binding to the CSP is a key factor for enantiorecognition. The effects of structural variance on separation were predicted. The steric bulkiness near the stereogenic centre in the analyte can also increase the separation. The different orientations of solute enantiomers for binding to the CSP when they are making the solute-CSP complex is the result of steric bulkiness near the stereogenic centre. The different orientation of solute enantiomers during the complexation with the CSP leads to enantiorecognition.

The matrix effect on separation was also reported. The longer spacer chain on the CSP increase the separation of sulphoxides.

# Acknowledegments

# References

1. T.J. Ward, **Anal. Chem. 72**, 4521 (2000).

2. K.B. Lipkowitz, **J. Chromatogr. A, 906**, 417 (2001).

3.  S. Weinstein, L. Leiserowitz and E. Gil-Av, **J. Am. Chem. Soc. 102**, 2768 (1980).

4.  K.B. Lipkowitz, D.J. Malik, and T. Darden, **Tetrahedron Lett. 27**, 1759 (1986).

5.  J.H. Pirkle, J.M. Finn and B.C. Hamper, **J. Am. Chem. Soc. 103**, 3964 (1981).

6.  W.H. Pirkle and J.M. Finn, **J. Org. Chem. 46**, 2935 (1981).

7.  W.H. Pirkle and M.H. Hyun, **J. Org. Chem. 49**, 3043 (1984).

8.  W.H. Pirkle, M.H. Hyun and B. Bank, **J. Chromatog. 316**, 585 (1984).

9.  K.B. Lipkowitz, J.M. Landwer and T. Darden, **Anal. Chem. 58,** 1611 (1986).

10. K.B. Lipkowitz, D.A. Demeter, C.A. Parish and J.M. Landwer, **J. Comput. Chem. 87,** 53 (1987).

11. K.B. Lipkowitz, D.A. Demeter, R. Zegara, R. Larter and T. Darden, **J. Am. Chem. Soc. 110,** 3446 (1988).

12. K.B. Lipkowitz, D.A. Demeter, C.A. Parish and T. Darden, **Anal. Chem. 59,** 1731 (1987).

13. W.H. Pirkle and T.C. Pochapsky, **J. Am. Chem. Soc. 109**, 5975 (1987).

14. S. Topiol, M. Sabio, J. Moroz, and W.B. Caldwell, **J. Am. Chem. Soc. 110**, 8367 (1988).

15. W.J. Hehre, R.F. Stewart and J.A. Pople, **J. Chem. Phys. 51,** 2657 (1969).

16. M.S.J. Dewar, E.G. Zoebisch, E.F. Healy and J.J.P. Stewart, **J. Am. Chem. Soc. 107,** 3902 (1985).

17. S. Topiol and M. Sabio, **J. Chromatog. 461,** 129 (1989).

18. M. Sabio and S. Topiol, **Chirality 3**, 56 (1991).

19. M.G. Still and L.B. Rogers, **Talanta 36,** 35 (1989).

20. T.D. Booth and I.W. Wainer, **J. Chromatog. 737**, 157-169 (1996).

21. A.M. Edge, D.M. Heaton, K.D. Bartle, A.A. Clifford and P. Myers, **Chromatog. 41,** 161 (1995).

22. HyperChemTM, Release 4, Hypercube, Waterloo, Ontario, Canada.

23. W.H. Pirkle, D.W. House and J.M. Finn, **J. Chromatog., 192,** 143 (1980).

24. K.B. Lipkowitz, B. Baker, and R. Zegarra, **J. Comput. Chem., 10**, 718-732 (1989).

25. C.E. Dalgleish, **J. Am. Chem. Soc. 137**, 3940 (1952).

26. S.G. Allenmark, "Chromatographic Enantioseparation Methods and Applications", Ellis Horwood, Chichester, 1988.

27. Dmoch, R. and Bartle, K.D.: 18. International Symposium on Capillary Chromatography, Riva del Garda, Italy, May 20-24, pp:1900-1904, (1996).

28. W.H. Pirkle and T.C. Pochapsky, **Chem. Rev. 89,** 347 (1989).

29. I.W. Wainer and M.C. Alembik, **J. Chromatog. 358**, 85 (1986).

30. I.W. Wainer and M.C. Alembik, **J. Chromatog. 367**, 59 (1986).